J. Fluid Mech. (1990), *vol.* 212, *pp.* 309–335
Printed in Great Britain

Emptying filling boxes: the fluid mechanics of natural ventilation

By P. F. LINDEN, G. F. LANE-SERFF AND D. A. SMEED
Department of Applied Mathematics and Theoretical Physics, University of Cambridge, Silver Street, Cambridge CB3 9EW, UK

(Received 30 June 1989)

This paper describes the fluid mechanics of the natural ventilation of a space connected to a large body of stationary ambient fluid. The flows are driven by buoyancy differences between the interior and exterior fluids. Connections with the ambient fluid are high level and low level openings. Two main forms of ventilation are identified: mixing ventilation and displacement ventilation. Mixing ventilation occurs when the incoming ambient fluid mixes with the fluid within the space, as is the case if dense fluid enters through a high level inlet. In this case vertical stratification is weak. Displacement ventilation occurs when dense fluid enters at low levels and displaces the lighter fluid within the space out through high level openings. A strong stable stratification develops in this case, and there is little mixing between the incoming fluid and that in the interior. Both of these modes of ventilation are studied theoretically and the results are compared with laboratory experiments. Transient draining flows which occur when a space initially contains fluid of a density different from the ambient are examined.

The presence of internal sources of buoyancy allows steady states to be established, and the effects of point, line and vertically distributed sources are studied. These steady states are extensions of filling box models, with the addition of continuous exchange of fluid with the environment outside the space. A major result of this work is that the form of the stratification within the space depends on the entrainment caused by the convective elements (plumes) produced by the buoyancy sources, but is independent of the strength of the sources. The strength of the stratification and the magnitudes of the velocities do, however, depend on the source strength. The effects of opening size(s) and configurations are determined, and criteria for producing a particular stratification within the space are established. Applications of this work to the ventilation of buildings are presented.

1. Introduction

Natural ventilation is the exchange of fluid between the interior of some space and its exterior environment when the flow is produced by naturally occurring pressure differences. It is the means by which most houses are ventilated. The pressure differences are produced by the action of the wind or by temperature differences between the internal and external air. The purpose of ventilation is to remove air contaminated with excess heat, humidity, carbon dioxide, toxins and other unwanted substances, and to provide clean air at a comfortable temperature and humidity. Modern buildings are very 'tight', both in terms of small rates of air infiltration through cracks in the building skin, and also in terms of high thermal insulation and low heat loss. The main problem to be overcome by the ventilation systems in such

buildings is to keep the air temperature experienced by the occupants from rising above a comfortable level. Mechanical ventilation is costly to install and maintain, and there have been cases where the ventilation has failed to provide clean air, resulting in the so-called 'sick building' syndrome.

In the last few years, as a result of these drawbacks with mechanical ventilation systems, architects have returned to natural ventilation (Penz 1983), particularly in buildings where large temperature differences may occur. One example, which is currently fashionable, is the ventilation of atria. These are popular as a means of providing a well-lit, covered environment within a group of buildings such as a shopping complex. Atria, typically, enclose quite tall, open plan spaces, and with the high solar gains during the summer and convective cooling during the winter, the design of an efficient ventilation system is a complex task. Connections to the outside air may occur at a number of levels, and significant thermal stratification has been measured within atria (Penz 1986).

The purpose of this paper is to elucidate the fluid mechanics of the processes that can occur in naturally ventilated systems. Much of the work is motivated by the need to obtain a deeper understanding of the fluid flows within buildings caused by temperature differences, and the cases we consider reflect this motivation. It also has applications to other problems of practical interest such as the accumulation of gas following a gas leak and the strategy for the efficient flushing of a space. Another example, on a different scale, concerns the replenishment of magma chambers with molten magma.

Attention is restricted to flows driven by temperature or other buoyancy differences between the interior and the exterior fluid. The effects of wind, while undoubtedly important to building design, are excluded from the discussion, although a few remarks will be made in the final section of the paper. Two main cases are considered. Firstly, the transient flow which develops when the interior is initially at a different temperature to the exterior and one or more vents are opened is examined. Secondly, the effects of constant internal heat sources such as heating equipment, machinery, occupants (about 100 W per sedentary person) or sunlight heating interior surfaces (a maximum value of approximately 800 W m^{-2} at mid-latitudes under glass) are studied.

In both of these cases, the ventilation flows can be divided into two basic categories called *mixing ventilation* and *displacement ventilation*. In a mixing system the fresh air is introduced in such a way as to mix throughout the ventilated space. The inlets and outlets are arranged so that relatively cool air enters at high levels or relatively warm air enters at low levels within the space, so that buoyant convection produces the mixing; see figure 1 (*a*). In some cases a single vent may act as both inlet and outlet. In displacement ventilation relatively cool, and thus dense, air is introduced into the space near the floor and the warm air is extracted near the ceiling; see figure 1 (*b*). In this case a stable stratification is produced by the ventilation flow and vertical mixing is minimal. In reality many systems are intermediate between these two, but we shall show that most cases can be discussed in terms of one or other of these categories.

A mathematical model of this flow is described in which the effects of internal sources of heat are modelled as turbulent plumes, using the entrainment assumption of Morton, Taylor & Turner (1956). Displacement flows are discussed in §2, and mixing flows are analysed in §3. Laboratory experiments designed to illustrate and compare with the theory are described in §4, and the results are given in §5. The

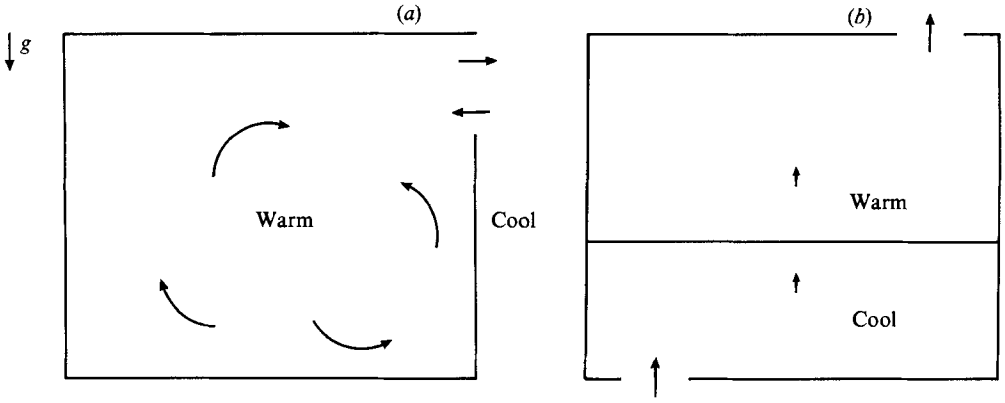

FIGURE 1. (*a*) Mixing ventilation and (*b*) displacement ventilation. In both cases warm air leaves the space near the ceiling: in the former cool air enters near the ceiling, mixing up the air in the space as it falls; in the latter cool air enters near the floor, displacing warm air upwards with little mixing.

applications of the work to building ventilation, and scaling laws for model studies, are discussed in §6, and the conclusions are given in §7.

2. Mathematical model for displacement flows

Consider a turbulent, entraining plume rising from a source of buoyancy in a closed space. The light fluid in the plume will reach the ceiling, spread to the sidewalls and descend in the space between the sidewalls and the plume, as shown in figure 2(*a*). Since the upper part of the plume is now surrounded by, and thus entrains, lighter fluid the plume becomes lighter than if it were surrounded by fluid of the initial density, and a stable stratification develops in the fluid. This 'filling box' mechanism was first described in detail by Baines & Turner (1969) and has also been studied by Worster & Huppert (1983); figure 2(*b*), taken from the latter paper, shows the density profiles in the region outside the plume at successive times.

If openings are now made in the floor and ceiling of the space, the layer of buoyant fluid near the ceiling will drive a flow through the openings, since the hydrostatic pressure difference between the top and bottom of the layer will be smaller than that between the same heights in the denser fluid outside the space. It will be assumed that the difference between the density of the ambient fluid, ρ, and that of the fluid in the space, $\rho-\Delta\rho$, is relatively small, and we shall write $g' = g\Delta\rho/\rho$ for the reduced gravity. The flux driven through the openings will depend, in general, on some integral of g' throughout the space, $I[g'\text{: space}]$ say. There will be inflow through the openings at the floor and outflow through the openings at the ceiling, imposing a general vertical flow within the space. After some time a steady state will be achieved: there will be a constant level below which all the fluid outside the plume will be dense ambient fluid and above which the fluid will be lighter than ambient, as shown in figure 3. Within the plume, fluid will be rising, and outside the plume the horizontal component of velocity will be towards the plume, because of entrainment by the plume. Above the interface and outside the plume the vertical component of velocity will be downward, decreasing to zero as the interface is approached, while below the interface the vertical component of velocity will be upward, again

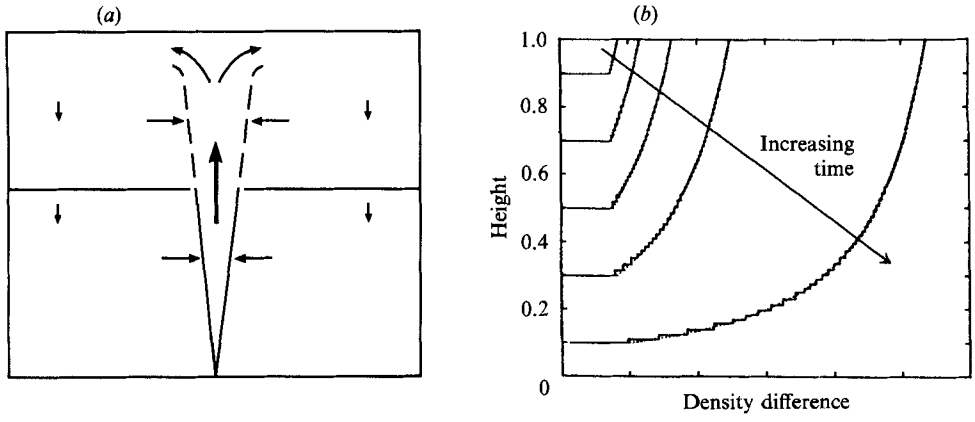

FIGURE 2. (*a*) A plume rising from a source of buoyancy in a closed box. The plume entrains fluid from the surroundings as it rises. On reaching the ceiling the buoyant fluid spreads and then descends, with a front between the buoyant fluid and the fluid still at the original density. (*b*) Calculated density profiles in the region outside the plume at successive times. Note the sharp jump in density across the descending front and the variation in density between the front and the ceiling, with most of the density change in the region just above the front. (The steps in the density profile are an artefact of the numerical scheme, the expected profile would be smooth except at the front.) This figure is taken from Worster & Huppert (1983).

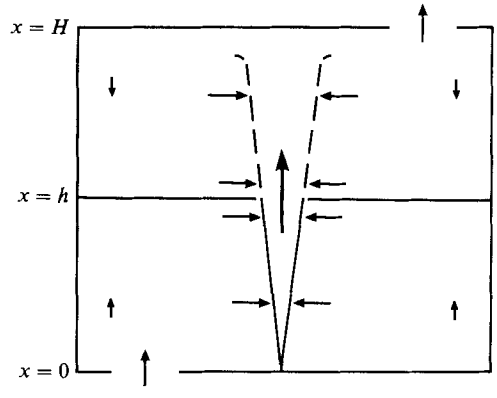

FIGURE 3. Steady displacement flow in a box with an internal source of buoyancy. The rising plume entrains fluid both above and below the interface. Outside the plume and below the interface the vertical component of velocity is upward: outside the plume and above the interface the vertical component of velocity is downward. Buoyant fluid leaves the space through the upper opening and ambient fluid enters through the lower opening.

decreasing to zero at the interface. Note that, although the interface is stationary, there is a horizontal component of velocity towards the entraining plume there, and the fluid at the interface is constantly refreshed from above and below. We shall write x for the vertical distance from the floor, with the steady interface at $x = h$ and the ceiling at $x = H$.

The vertical volume flow rate through any horizontal plane must be constant so that, in particular, the volume flow rate through the openings, F say, must be equal to the volume flow rate in the plume at the interface height, M_i say. Also the buoyancy flux through the upper opening, $g'_u F$ say, must equal the buoyancy flux in the plume at the interface height, $G'_i M_i$ say. Thus g'_u at the upper opening must equal G'_i in the plume at the interface height so that g' must have the same value

throughout the region above the interface, both inside and outside the plume, and therefore the plume is a momentum jet in this region. For plumes in an unstratified ambient fluid the buoyancy flux, $G'(x,B)M(x,B)$, is constant, equal to the buoyancy flux, B, at the source; $G'(x,B)$, the value of g' within the plume, decreases with height x, and $M(x,B)$, the volume flux within the plume, increases. Here 'top-hat' profiles for the density and velocity across the plume have been assumed. To find the steady interface height, and thus determine the flow in the space, we match the volume flux within the plume with the volume flux that is driven through the openings by the layer of light fluid above the interface. The density of this light fluid is determined by equating it with the density of the plume fluid at the interface height. Using $g'(x)$ to denote the value of g' in the region above the interface and outside the plume, we can write this argument as follows:

equating volume fluxes $$F = M_\mathrm{i}, \tag{2.1a}$$

where $$F \equiv F(I[g'(x): h < x < H]) \quad \text{and} \quad M_\mathrm{i} \equiv M(x = h, B);$$

equating buoyancy fluxes $$g'_\mathrm{u} F = G'_\mathrm{i} M_\mathrm{i}, \tag{2.1b}$$

where $$g'_\mathrm{u} \equiv g'(x = H) \quad \text{and} \quad G'_\mathrm{i} \equiv G'(x = h, B).$$

Hence $$g'(x) = \begin{cases} G'_\mathrm{i} = G'(x = h, B), & h \leqslant x \leqslant H \\ 0, & 0 \leqslant x < h. \end{cases} \tag{2.1c}$$

Having determined $g'(x)$, we find that $I = G'_\mathrm{i}(H-h)$ and we can substitute this into the expression for F and equate F with M_i to find h. To solve the problem, then, we need to know the flux driven through the openings by a layer of light fluid of uniform density as a function of the depth of the layer and g', and also the properties of a plume (in particular the volume flux and G') as a function of the distance above the source. We treat this problem in two parts as follows.

2.1. *Simple draining flows*

Consider the emptying of a space initially filled with relatively light fluid, of uniform density, through a pair of openings, one in the ceiling of area a_1 and one in the floor of area a_2. We shall write u_1 and u_2 for the velocity of the fluid through these openings and H for the (constant) height of the ceiling from the floor. It will be assumed that the incoming fluid does not mix with the fluid in the space but forms a layer of increasing depth, h, on the floor of the space, and that the horizontal area of the space, S (independent of height), is much larger than the area of either opening so that the velocity of the interface between the dense and light fluid is negligible: see figure 4.

At some horizontal level, between the interface and the ceiling, the hydrostatic pressure will be equal inside and outside the building. This level is known as the 'neutral level'. Writing z for the vertical distance between this level and the interface, and using Bernoulli's theorem we have

$$u_1^2 = 2g'(H-h-z), \tag{2.2a}$$

$$u_2^2 = 2g'z. \tag{2.2b}$$

After flowing through an orifice the flow will contract and so these equations should only be applied to the velocities and areas after contraction. Also the flows are not dissipationless so Bernoulli's theorem is not strictly applicable. In particular, there will be a drop in head following the streamline through the inlet and we can use the

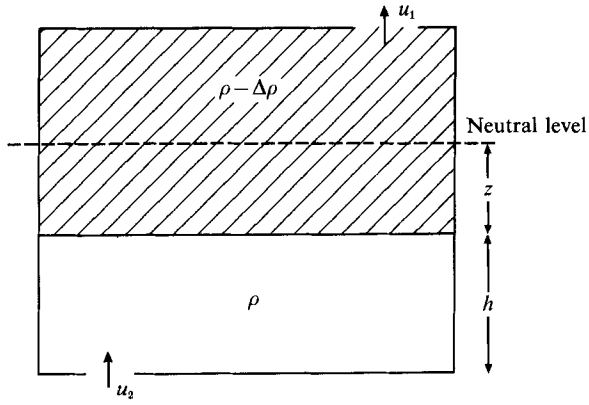

FIGURE 4. Displacement flow from a box initially containing fluid of density $\rho-\Delta\rho$. The velocity of the fluid through the openings is shown, together with the area of each opening. The horizontal dashed line denotes the 'neutral level' at which the pressure inside and outside the space are equal.

momentum theorem (see, for example, Batchelor 1967, chapter 5) to replace equation (2.2*b*) with

$$u_2^2 = 2cg'z, \tag{2.2c}$$

where c is a constant lying between one half, for a sharp expansion at the inlet (with $a_2 \ll S$), and unity, for a perfectly smooth expansion.

If the fluid is incompressible the volume flux into the space must equal the flux out, so that

$$F = u_1 a_1 = u_2 a_2. \tag{2.3}$$

Eliminating z from (2.2) and using (2.3) gives

$$F = A^*(g'(H-h))^{\frac{1}{2}}, \tag{2.4a}$$

where

$$A^* = \frac{a_1 a_2}{(\frac{1}{2}(a_1^2/c + a_2^2))^{\frac{1}{2}}} \tag{2.4b}$$

is an 'effective area' of the openings. Note that if $a_1 < a_2$ then $A^* < a_1\sqrt{2}$, while if $a_1 > a_2$ then $A^* < a_2\sqrt{(2c)}$. Thus A^* is largely dependent upon the smaller of a_1 and a_2, so increasing the size of the openings at one level once they are already larger than the openings at the other level achieves little extra flow. The buoyancy flux, B, is given by

$$B = Fg' = A^*(H-h)^{\frac{1}{2}}g'^{\frac{3}{2}}. \tag{2.5}$$

Now

$$\frac{\mathrm{d}h}{\mathrm{d}t} = \frac{F}{S}, \tag{2.6}$$

and so, if $h = 0$ when $t = 0$

$$\frac{h}{H} = 1-\left(1-\frac{t}{t_E}\right)^2, \tag{2.7}$$

where the time, t_E, for the space to empty is given by

$$t_E = \left(\frac{2S}{A^*}\right)\left(\frac{H}{g'}\right)^{\frac{1}{2}}. \tag{2.8}$$

2.2. *Effects of continuous sources of buoyancy at one level*

The second part of the problem is to determine the effects of continuous sources of buoyancy. We consider particular sources of buoyancy, and begin with a point source. The equations for a buoyant plume in a large body of stationary, unstratified, ambient fluid are given in Morton *et al.* (1956). From equations (4) of that paper the buoyancy and volume fluxes, B and M, and g' can be recovered, thus

$$B = G'M = \text{constant}, \tag{2.9a}$$

$$M(x,B) = C(Bx^5)^{\frac{1}{3}}, \tag{2.9b}$$

$$G'(x,B) = (B^2x^{-5})^{\frac{1}{3}}/C, \tag{2.9c}$$

where x is the vertical distance from the source (which we shall assume to be on the floor), and $C = \frac{6}{5}\alpha(\frac{9}{10}\alpha)^{\frac{1}{3}}\pi^{\frac{2}{3}}$ is a universal constant dependent on the entrainment constant α.

Equating volume fluxes from (2.4) and (2.9) we find

$$A^*(g'(H-h))^{\frac{1}{2}} = CB^{\frac{1}{3}}h^{\frac{5}{3}}. \tag{2.10}$$

Writing ξ for h/H and equating g' with $G'(x = h, B)$ from (2.9) we obtain

$$\frac{A^*}{H^2} = C^{\frac{3}{2}}\left(\frac{\xi^5}{1-\xi}\right)^{\frac{1}{2}}, \tag{2.11a}$$

$$g'(h \leqslant x \leqslant H) = G'(x = h, B) = (B^2h^{-5})^{\frac{1}{3}}/C. \tag{2.11b}$$

Note that (2.11a) is a relation between two geometric quantities: the height of the interface as a fraction of the ceiling height and the area of the openings non-dimensionalized with respect to the square of the ceiling height. There is no dependence of the interface height on the strength of the source, nor on the floor area S.

Consider now n equal sources all on the same vertical level and sufficiently far apart that their plumes do not interact. It is clear that multiplying the area of the openings by the number of plumes will result in the same interface height with the same density difference between the incoming air and the air above the interface. Thus for multiple sources

$$\frac{1}{n}\frac{A^*}{H^2} = C^{\frac{3}{2}}\left(\frac{\xi^5}{1-\xi}\right)^{\frac{1}{2}}. \tag{2.12}$$

It is a simple matter to adapt this analysis for a two-dimensional line plume. For such a plume the volume flux per unit length, M_L, and g' are given in terms of the (constant) buoyancy flux per unit length, B_L, by

$$M_L(x,B_L) = DB_L^{\frac{1}{3}}x, \tag{2.13a}$$

$$G'(x,B_L) = B_L^{\frac{2}{3}}/(xD), \tag{2.13b}$$

where $D = (2\alpha)^{\frac{2}{3}}$ is a universal constant, dependent on the entrainment constant α. Writing A_L^* for the effective area of the openings per unit length and equating volume fluxes and g' as before, we find

$$\frac{A_L^*}{H} = D^{\frac{3}{2}}\left(\frac{\xi^3}{1-\xi}\right)^{\frac{1}{2}}, \tag{2.14a}$$

$$g'(h \leqslant x \leqslant H) = G'(x = h, B_L) = B_L^{\frac{2}{3}}/(hD). \tag{2.14b}$$

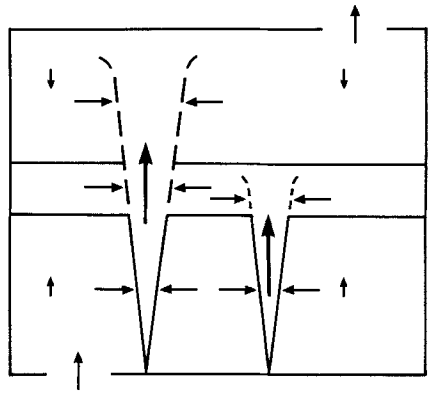

FIGURE 5. Steady displacement flow in a box containing two sources of buoyancy of differing strengths. There are two layers of relatively light fluid above a layer of ambient fluid. The middle layer will have the same density as that of the weaker plume at the lower interface, the upper layer will have the same density as that of the stronger plume at the upper interface. Note, however, that the stronger plume entrains fluid lighter than ambient where it passes through the middle layer.

Note that multiple line sources can be treated as for multiple point sources, and also that a line source against a vertical wall can be approximated as half of a line source whose buoyancy flux is twice that of the true source.

The position of the lower openings does not alter the position of the interface, provided they are below the interface, nor will their position affect the flow in the plume or plumes, though it may affect the vertical velocity in the region outside the plume or plumes below the interface. Plumes from sources other than points or lines can be approximated by considering the source to be at the apparent origin of the buoyant plume shape to which all plumes tend. Thus H should be interpreted as the distance of the ceiling from this apparent origin. Note that the part of the space below the interface does not influence the flow rate or the position of the interface. There will be a more detailed discussion of plumes and entrainment in the concluding section. Where there are unequal multiple sources the density difference between each plume and the incoming fluid will be different for different plumes at any given height. The steady solution will have layers of decreasing density towards the ceiling with sharp interfaces between the layers; this situation is sketched in figure 5. In general, then, the flow from a distribution of sources will be complex. However, all entraining flows of this type have the important property that the volume flux increases with height while the density difference decreases. A thicker layer of lighter fluid will drive a larger volume flux through the openings, and so a displacement flow will always be set up with a layer or layers of light fluid above an interface, below which there will be entraining plumes flushing the lower region.

In the analysis above it has been assumed that the sources of buoyancy were all below the level of the lowest interface. This need not be the case and we shall now investigate the flow due to a regular arrangement of sources spread over the full height of the space.

2.3. *Effects of vertically distributed sources*

Consider the case in which a source of buoyancy is uniformly distributed over a vertical wall. In this situation we would expect a plume to form against the wall and the system to adjust to a steady state in a manner similar to that described for point and horizontal line sources above. However, if an interface forms at some height

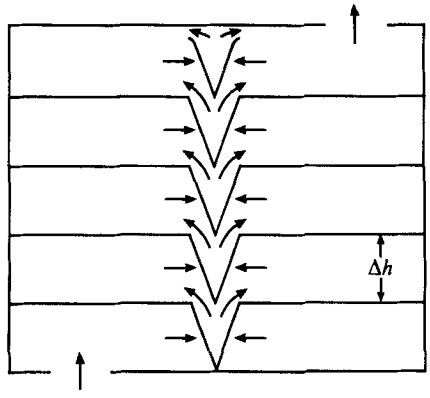

FIGURE 6. Steady displacement flow in a box containing a vertically distributed source of buoyancy. There are many layers of decreasing density approaching the ceiling. A plume starts at the bottom of each layer, entraining surrounding fluid as it rises. The density of each layer is equal to that of the plume from the layer below at the interface between the layers.

there will be a source of buoyancy above the interface and a second plume will form. This gives rise to the possibility of stratification more complicated than the two-layer profiles discussed above. At any level where the volume flux in the plume is not equal to the volume flux out of the box there must be a net vertical motion exterior to the plume, and for the state to be steady fluid elements exterior to the plume must move along surfaces of constant density (assuming diffusion to be negligible). This suggests that the steady state will have a layered density profile with the interfaces at levels at which the volume flux in the plume is exactly equal to the flux through the box. Such a state is depicted in figure 6.

The theory described above for point and horizontal line sources can be easily extended to consider this case, if we make the following idealizations: (i) at each level the plume is well mixed and of uniform density; (ii) if the density of the plume is equal to the density of the fluid exterior to the plume at the same height, then all fluid from the plume detrains at that level and a new plume starts immediately (see figure 6).

Again the problem is solved by equating the volume flux F through the box due to the difference in hydrostatic pressure between the inside and outside of the space and the volume flux across each interface within the turbulent plumes M_i. This requires that the depth of each layer, with the exception of the uppermost layer, must be the same. We shall write Δh for the layer depth and $\Delta g'$ for the change in buoyancy between adjacent layers.

The relation (2.4) for the volume flux, F, out of the box may be generalized for arbitrary density profiles as follows:

$$F = A^* \left(\int_0^H g' \, \mathrm{d}z \right)^{\frac{1}{2}}. \tag{2.15}$$

If we make the additional assumption that the top layer is the same depth as the other layers then

$$F = A^* (\tfrac{1}{2} \Delta g' \Delta h N (N+1))^{\frac{1}{2}}, \tag{2.16}$$

where N is the number of interfaces.

Experimentally it is easier to consider a vertical line source than a planar source and so we consider here the case of a vertical line source with buoyancy flux B_H per

unit length. It can be shown that, if the entrainment assumption is valid, g' and the volume flux within a plume are given by

$$G'(x, B_H) = (2B_H^2/\pi^2)^{\frac{1}{3}}(\alpha x)^{-1} \quad \text{and} \quad M = (\tfrac{1}{2}\pi^2 B_H)^{\frac{1}{3}}\alpha x^2, \tag{2.17}$$

where x is the height above the base of the source.

Now substituting $x = \Delta h$ in (2.16) and (2.17) and equating F with M_i we obtain an expression for the number of layers,

$$N(N+1)^5 = \alpha^3\pi^2 \frac{H^4}{A^{*2}}. \tag{2.18a}$$

The change in g' across each layer is

$$\Delta g' = G'(x = \Delta h, B_H) = (2B_H^2/\pi^2)^{\frac{1}{3}}(\alpha \Delta h)^{-1}. \tag{2.18b}$$

Note that increasing the area of the openings decreases N and hence the volume flux F increases only slowly. The applicability of the entrainment assumption is uncertain, particularly to the case of a heated wall. However, if the volume flux increases with height and g' decreases with height we should expect layers to form but the size of the layers will be different.

3. Mathematical model for mixing flows

In the previous section it was assumed that there was a clear distinction between openings through which fluid flowed into the space and those through which fluid flowed out of the space. Consider now a single opening high in a vertical wall of the space. In this case the neutral level at which the pressure is equal inside and outside the space will be at approximately half the height of the opening, and there will be a controlled exchange flow through the window as described, for example, by Dalziel (1988) and Linden & Simpson (1985), giving a volume flux through the window of

$$F = kA(g'd)^{\frac{1}{2}}, \tag{3.1}$$

where A is the area and d the height of the opening; g' is evaluated just inside the opening. For a vertical window the constant $k = 0.25$.

The dense incoming fluid will flow into the space, descending to the floor as a curved plume. The resulting flow will be an inverted version of the filling box process described above. Once the front of dense fluid has reached the level of the opening the stratification in the space will be weak and for this analysis it will be assumed that the fluid in the space is well mixed. Even if there are small openings at lower levels there may still be inflow through such an opening, and the following analysis will apply.

Consider first the case where the space is initially filled with light fluid and an inlet is opened. Here $\Delta\rho$ will be the density difference between the space and the ambient air, V the volume of the space and subscript 0 will denote initial values of quantities at time $t = 0$. From conservation of mass we find

$$\frac{\mathrm{d}g'}{\mathrm{d}t} = -\frac{g'F}{V} = -\frac{kAd^{\frac{1}{2}}g'^{\frac{3}{2}}}{V}. \tag{3.2}$$

Integrating (3.2) gives

$$\frac{g'}{g'_0} = \left(1 + \frac{t}{\tau}\right)^{-2}, \tag{3.3a}$$

where the mixing timescale τ is given by

$$\tau = \frac{2V}{kA}(g'_0 d)^{-\frac{1}{2}}. \tag{3.3b}$$

Defining $t_{\frac{1}{2}}$ to be the time for g' to reduce to half its initial value,

$$t_{\frac{1}{2}} = (\sqrt{2}-1)\tau. \tag{3.4}$$

It is also possible to have an exchange flow with a single opening in the horizontal surface of the ceiling. The flow in this case differs from the previous case of a window in a vertical wall since there is no preferred arrangement of the incoming and outgoing fluid. On dimensional grounds one again expects the flux through such an opening to be given by equation (2.1), where here d is the longest length of the opening and k a constant dependent on the opening shape. For circular openings Epstein (1988) found a value of $k = 0.055$ and Brown, Wilson & Selvason (1963) give $k = 0.051$ for a square window where d in (3.1) is taken to be the diagonal. Compared with the equivalent value of one quarter for openings in a vertical wall this shows that the ceiling opening is only about one fifth as efficient as a window.

When there are sources of buoyancy in the space a steady state will be achieved in which the buoyancy flux through the opening is equal to that produced by the internal sources, B say. The arrangement of the sources within the space is unimportant, thus

$$B = Fg' = kAd^{\frac{1}{2}}g'^{\frac{3}{2}}_{\mathrm{E}}, \tag{3.5a}$$

and so

$$g'_{\mathrm{E}} = \left(\frac{B}{kAd^{\frac{1}{2}}}\right)^{\frac{2}{3}}, \tag{3.5b}$$

where g'_{E} is the value of g' at the level of the openings in the steady state.

The incoming ambient fluid creates a descending plume within the box. If the ascending and descending plumes are sufficiently far apart that they do not interact a steady two-layer stratification will be set up within the space. The density of the lower layer will be that of the descending plume at the interface, while the density of the upper layer will be that of the ascending plume at the interface. This arrangement is shown in figure 7. The value of g' for the upper layer is that given for g'_{E} in (3.5*b*). The volume flux in the ascending plume at the interface must equal that for the descending plume at the interface. Noting that the fluid surrounding the plumes is of different density in the two layers, and is in both cases different from the density of the fluid outside the space, we can calculate the position of the interface and the density of the two layers in a similar manner to that described earlier for displacement flows.

If the area of the openings is small compared to the square of the height of the box then we can model the openings as N_{o} plumes each originating from a point source on the top of the box and each of buoyancy flux B/N_{o}, where B is the total buoyancy flux from the N_{s} point sources on the bottom of the box and N_{o} is the number of openings. If the interface is situated at a height h above the bottom of the box then, equating the volume flux of the ascending plumes at the height of the interface with that of the descending plumes at the same level, we have

$$CN_{\mathrm{s}}\left(h^5\frac{B}{N_{\mathrm{s}}}\right)^{\frac{1}{3}} = CN_{\mathrm{o}}\left((H-h)^5\frac{B}{N_{\mathrm{o}}}\right)^{\frac{1}{3}}, \tag{3.6}$$

and so

$$\frac{h}{H} = \frac{N_{\mathrm{o}}^{\frac{2}{5}}}{N_{\mathrm{s}}^{\frac{2}{5}}+N_{\mathrm{o}}^{\frac{2}{5}}}. \tag{3.7}$$

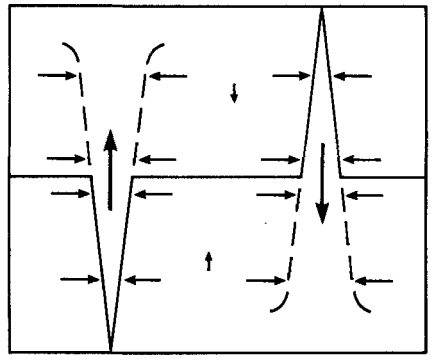

FIGURE 7. Steady flow in a closed box containing equal and opposite sources of buoyancy at the floor and ceiling. Both plumes entrain fluid from their surroundings. The vertical component of velocity in the region outside the plumes is downward above the interface and upward below. The density of the upper layer is equal to that in the rising plume at the interface: the density of the lower layer is equal to that in the descending plume at the interface.

Thus increasing the number of openings moves the interface nearer the top, and increasing the number of sources moves the interface nearer the bottom. The change in g' across the interface is given by

$$\Delta g' = \frac{(B^2/N_s^2 h^5)^{\frac{1}{3}}}{C}. \tag{3.8}$$

4. Experiments

The experiments were undertaken in a large reservoir of fresh water (0.6 m × 0.6 m × 13 m), within which was suspended a small Perspex box. Three boxes, each with a different geometry, have been used, but for most of the experiments to be discussed here a Perspex box 25 cm high, 30 cm long and 20 cm wide was used. A number of holes of diameter 1.8 cm or 5.5 cm were drilled in both the top and the bottom of the box. The holes could be opened or closed during the experiments using plastic plugs. The two other boxes are slightly larger in size and have more complex geometry. These are scale models of real buildings and have most of the openings in the sides rather than the top and bottom. Buoyancy-driven flows are created in the apparatus using brine which is denser than fresh water, therefore the buoyancy forces act downwards in contrast to the theoretical calculations in §§2 and 3 where the buoyancy forces act upwards. The large size of the reservoir ensured that fluid around the outside of the box remained at a constant density throughout the experiment.

Two types of experiments have been performed. In the first type the box is filled with brine of known density. Fluid within the box is thus initially of a uniform density greater than that of the fresh water in the reservoir. Plugs in either the bottom, or in the bottom and the top, are then opened and the resulting flow is examined. In the second type of experiment, fluid within the box is initially of uniform density equal to that of the ambient fluid. Brine is then introduced through a source in the box. This fluid descends forming a turbulent plume, and drives a flow within the box and an exchange with the exterior. The transient behaviour and the steady states are then examined for various configurations of openings. Three

different sources have been used. These were a 'point source', a small downward pointing tube covered in foam rubber; a 'horizontal line source', a perspex tube extending across the full width of the box (20 cm), in which holes are drilled at uniform intervals along the lower side; and a 'vertical line source', for which the perspex tube was vertical and holes were drilled on four sides of the tube at uniform intervals along the length. The length of the latter tube was equal to the height of the box (25 cm), and the tube was covered in foam. In all three cases the volume flux in the plume is, except within a few centimetres of the top of the box, much larger than volume flux from the source, so that the flow is driven by the flux of buoyancy and the source of volume is not significant. Typical values for the volume and buoyancy fluxes from the source are 20 $cm^3\ s^{-1}$ and 1000 $cm^4\ s^{-3}$.

The flows were visualized by adding dye to the brine and by use of the shadowgraph technique. Samples were taken using syringes to measure the density within the box and a conductivity probe was used in some of the experiments to measure the density profile.

5. Results

We shall mainly confine the discussion to the experiments in the simple rectangular box, though we shall occasionally refer to results from experiments in the scale models. The experiments fall into two categories of flow type, displacement flows and mixing flows; these can be further divided according to whether there were or were not internal sources.

5.1. *Displacement flows*

Displacement flows resulted when openings were made both in the top and in the bottom of the box.

Draining flows

In this first set of experiments fluid within the box was initially at a uniform density, and a number of plugs were removed from the top of the box. The experiment was then started by removing plugs at the bottom of the box. This resulted in an inflow through the top and an interface was established between the incoming fluid and the dense fluid below. The interface fell displacing the dense fluid from the box through the lower openings. The rate of descent of the interface was observed to decrease as it fell. The development of a typical experiment is shown in figure 8. In figure 9 the position of the interface is depicted as a function of time for a number of different experiments and compared with the predictions (equation (2.7)). The two curves on the graphs correspond to the cases $c = 1$ and $c = \frac{1}{2}$. The experimental results lie between the two curves as is expected. However, when the area of the openings in the top was smaller than the area of openings in the bottom the large velocity of the inflow resulted in a jet which caused the entrainment of buoyant fluid across the interface. In this case the interface descends significantly faster because of the greater density of the fluid above the interface (results from these experiments are not included on figure 9). When comparing experiments with significant entrainment with those in which very little mixing occurred, it should be noted that in the latter when the interface reaches the bottom there is no dense fluid within the box but in the former the box is not completely drained of dense fluid.

Very similar results were obtained using the other boxes. However, when the upper openings were not at the top of the box but some way down the wall, the amount of initial mixing was greater, and the interface was more diffuse.

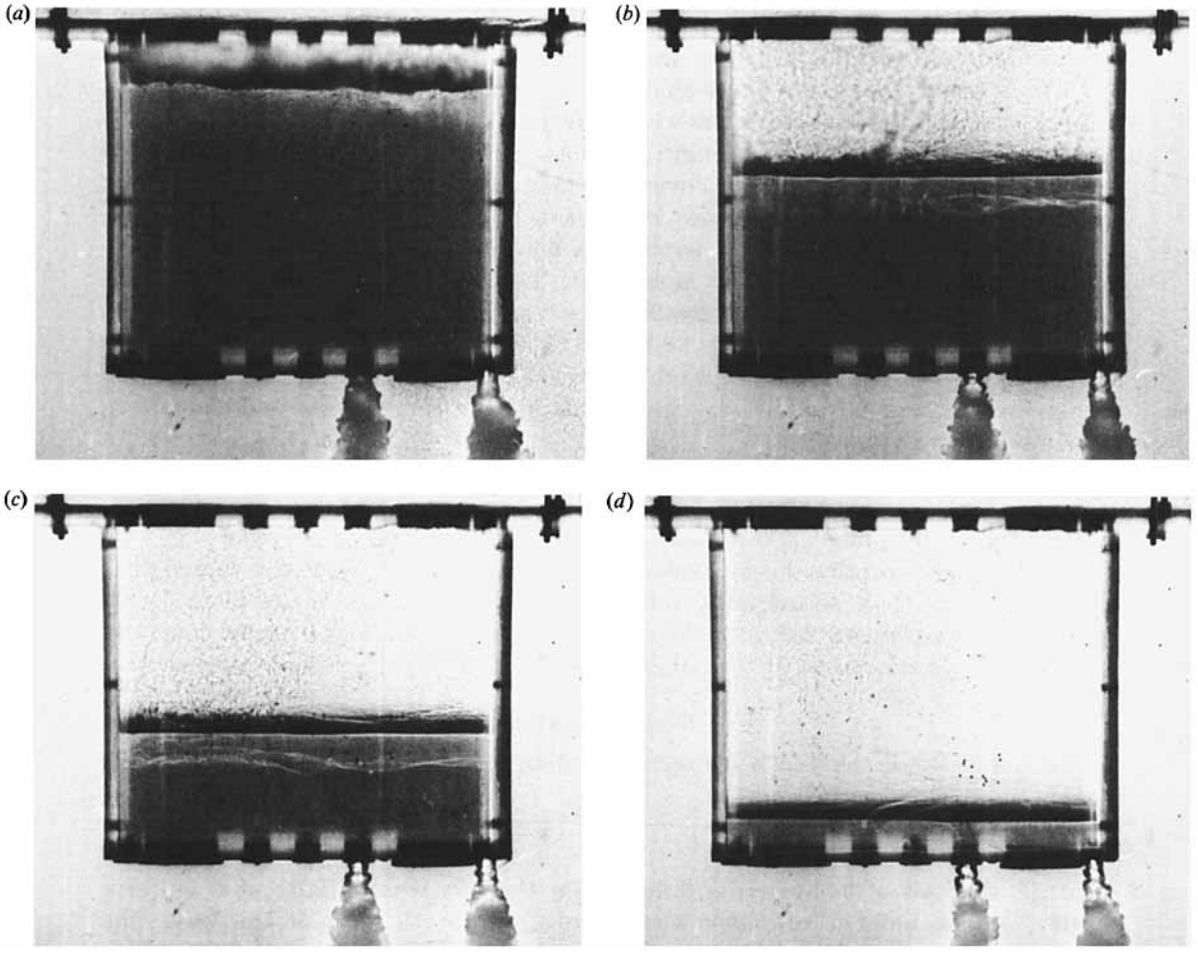

FIGURE 8. Displacement flow from a box initially containing dense fluid. The box was filled with dense fluid and lowered into the large reservoir of fresh water. Four large plugs (diameter 5.5 cm) were removed from the top of the box and the experiment was started by removing two small plugs (diameter 1.8 cm) from the bottom of the box. The photographs are at (*a*) $t/t_E = 0.07$, (*b*) 0.29, (*c*) 0.50 and (*d*) 0.86. The emptying time t_E is 139 s. Note the descending sharp interface between the clear, ambient fluid and the dark, dense fluid. These and subsequent photographs are of side views using the shadowgraph technique: the dense fluid is dyed.

Internal sources on one level

In this set of experiments openings at both the top and bottom were used, with internal sources of dense fluid at the top of the box (point source and horizontal line source).

Once an experiment is started a turbulent plume descends from the source. The plume entrains ambient fluid as it descends until it reaches the bottom of the box where it spreads horizontally. The dense fluid then begins to rise in the region outside the plume. This layer creates a flow through the box. There is outflow only through the lower openings and inflow only through the upper openings. A two-layer stratification is set up and the density of the lower layer increases as it deepens until a steady state is established in which the buoyancy flux out of the bottom balances

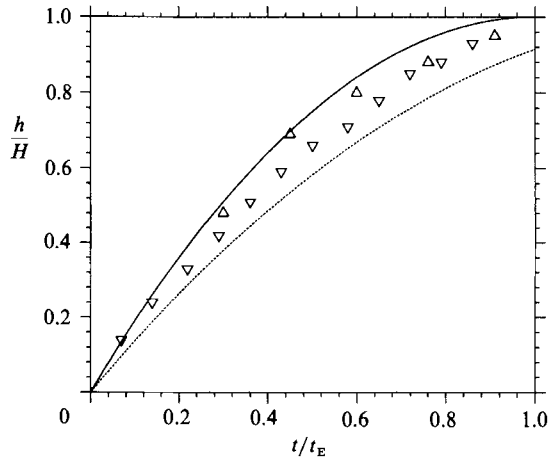

FIGURE 9. Emptying box by displacement flow. The dimensionless height, h/H, of the interface below the top of the box as a function of time. Results are shown for two experiments: (i) $a_1 = 23.8$ cm^2, $a_2 = 52.7$ cm^2 ($\triangle$); (ii) $a_1 = 5.1$ cm^2, $a_2 = 28.9$ cm^2 ($\triangledown$). The height h is scaled by H, the height of the box, and the time t is scaled by t_E (equation (2.8)) when c takes the value 1. The solid line is the prediction (2.7). The dashed line is the prediction for the case $c = \frac{1}{2}$ and $a_2 \ll a_1$.

that from the source. An example of such a flow is shown in figure 10 and corresponding density profile is shown in figure 11. In this steady state ambient fluid enters through the upper openings before being entrained into the plume and so transported across the interface.

The theory shows that the height of the interface is not dependent upon the buoyancy flux but only upon the geometry of the sources and openings (equation (2.11*a*)). However, if after a steady state is reached the buoyancy flux is reduced, there will be a transient state in which the interface is displaced. The buoyancy and volume fluxes of the plume are both reduced, but initially the volume flux out of the box remains the same, and so the interface begins to descend. This results in an increased volume flux across the interface (the volume flux in the plume increases with distance from the source) and decreased flux out of the box (as the hydrostatic pressure is reduced). Eventually the volume flux in the plume exceeds that out of the box and the interface rises to its original level: the equilibrium is re-established with a reduced density in the lower layer. Similarly, if the buoyancy flux is increased the interface rises initially before returning to its original position, but with an increased density in the lower layer.

The depth, h, of the upper layer and the value of g' in the lower layer are presented in figures 12 and 13 for point sources and line sources respectively, and compared with the theoretical predictions (equations (2.11) and (2.14)). Good agreement is found, both for point sources and line sources. As the value of A^* is increased the height of the interface, h, rises and the value of g' in the lower layer decreases. The rate of change of h and g' with A^* is very much smaller for large values of A^* than for small values of A^*; for example, in the case of a point source, when $A^*/H^2 = 0.01$, $h/H = 0.5$, but to raise h/H to 0.9 requires $A^*/H^2 = 0.10$.

Very similar results were obtained from the measurements using the scale models. In some of these cases, however, windows opened at levels close to the interface had exchange flows and not purely inflow or outflow. It was also found that with a very small area of openings at the top and a large area of openings at the bottom an

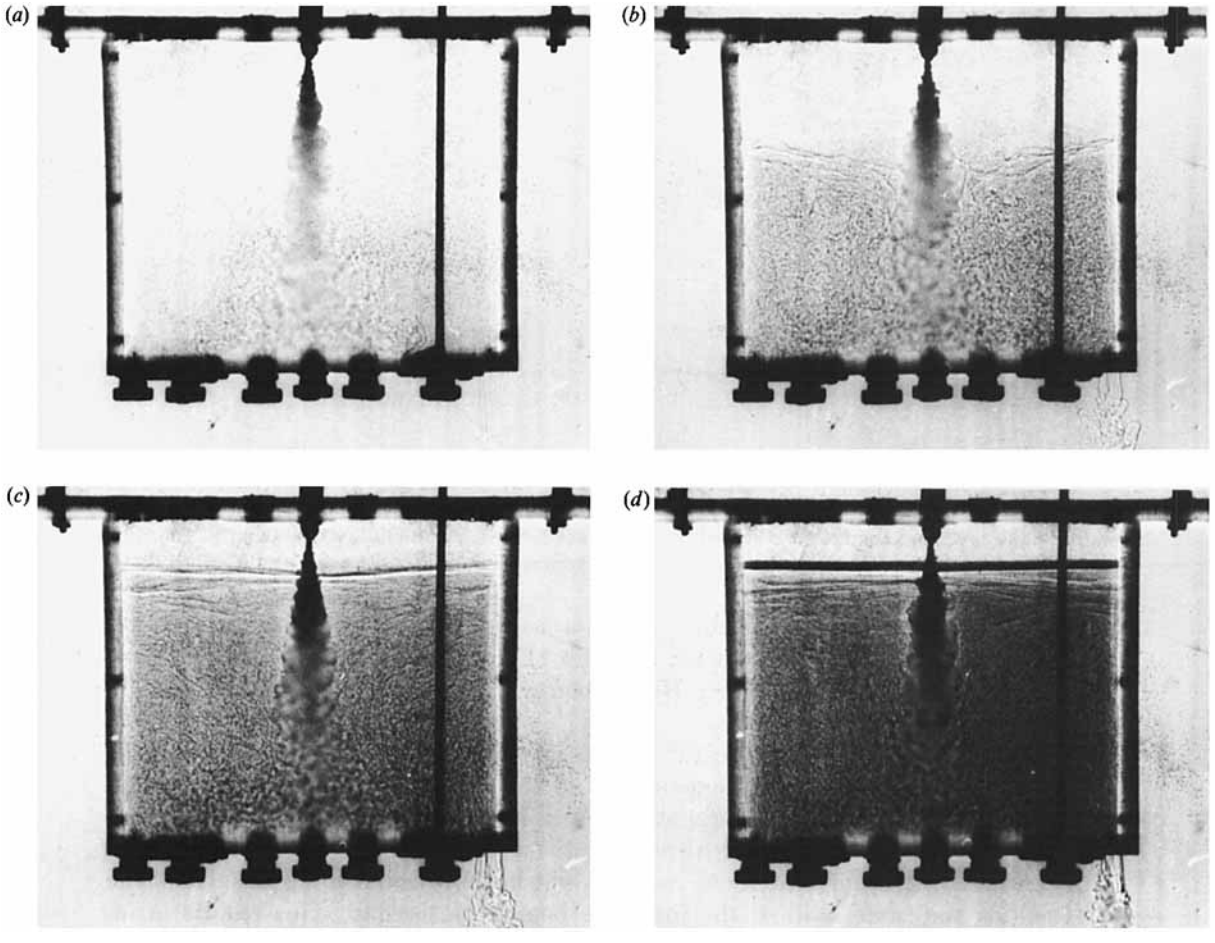

FIGURE 10. The development of steady displacement flow in a box with an internal source. The source here is a horizontal line source. Initially the box contains ambient fluid; four large plugs have been removed from the top and one small plug from the bottom. The experiment is started by starting the flow from the source. The photographs are at (*a*) $t = 10$, (*b*) 30, (*c*) 90 and (*d*) 240 s. Note the rising interface in the region outside the plume in the early part of the flow, the sharpening of the interface and the darkening of the fluid below the front later in the experiment. The dark, vertical tube in the box to the right of the plume is a conductivity probe: in this figure the measuring tip of the probe is near the bottom of the box.

exchange flow could be established through the lower vents causing the height of the interface to be raised. In this case the plume remains negatively buoyant in the lower layer.

Vertically distributed sources

We now discuss the results of experiments with displacement flows and vertical line sources. As for the previous case a steady flow is established after some time, with an upper interface above which all the fluid outside the plume consists of incoming fresh water. Below this level, however, the fluid is not at a uniform density as it had been when the source was entirely above the interface. Figure 14 shows a photograph of the flow in the steady state, and density profiles, obtained using a conductivity probe, are presented on figure 15. There is significant stratification

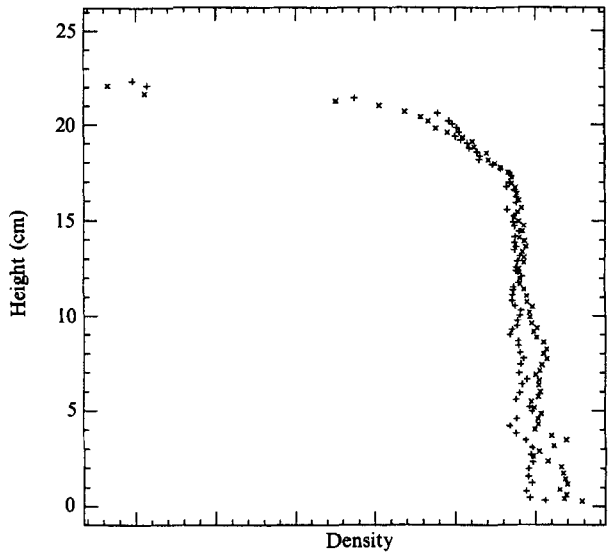

FIGURE 11. Density profile of a steady displacement flow with an internal source. This profile is from the experiment shown in figure 10 and was measured just after photograph (*a*) was taken. The density (which has not been calibrated) was measured using a vertically traversing conductivity probe (+, upward traverse; ×, downward traverse). Note the interface at 22 cm and the uniformity of the density below 17 cm.

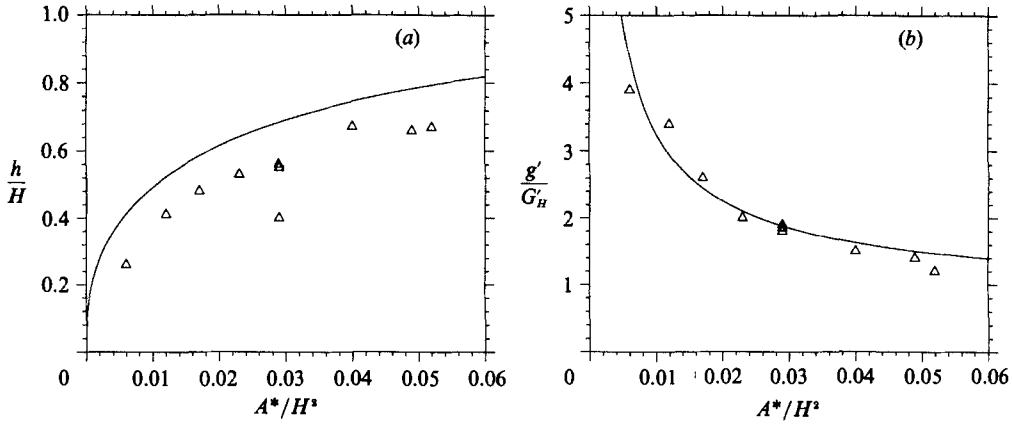

FIGURE 12. Displacement flows with a point source: (*a*) h/H *vs.* A^*/H^2; (*b*) g'/G'_H *vs.* A^*/H^2. The lines represent the predictions of (2.11*a*, *b*). The value $c = 1$ is used when calculating A^* and $G'_H \equiv G'(x = H, B)$ (see (2.9*c*)).

below the level of the interface and in some cases an indication of a second interface near the bottom, but this appears to be associated with the fluid from the plume spreading across the bottom as a gravity current. The theory, outlined in §2.3, would suggest the formation of perhaps three or four layers when the area of the openings is small, but this is not observed.

Several factors appear to contribute to this discrepancy. Firstly, the model is based on the entrainment assumption and on 'top-hat' profiles of density and velocity across the plume. In the experiments the plume was not fully turbulent and

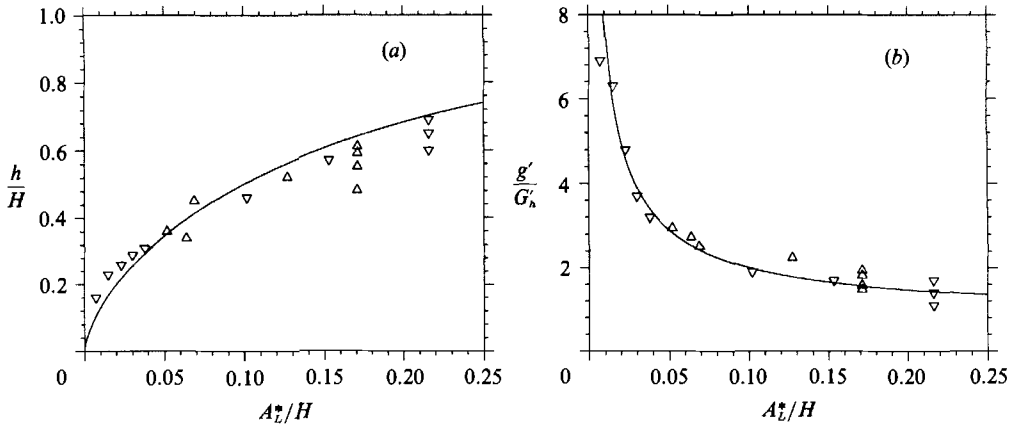

FIGURE 13. Displacement flows with a line source: (a) h/H *vs.* A_L^*/H; (b) g'/G'_H *vs.* A_L^*/H. The lines represent the predictions of (2.14*a*, *b*). The value $c = 1$ is used when calculating A^* and $G'_H \equiv G'(x = H, B)$ (see (2.13*b*)).

a laminar region adjacent to the source was present. This region did not mix with its surroundings and carried buoyancy across the interface. Secondly, a fairly strong circulation in the region outside the plume was observed. This caused a significant amount of vertical mixing, which is not accounted for in the model.

5.2. *Mixing flows*

These flows were observed in experiments in which openings in the bottom of the box only were used.

Draining flows

In this set of experiments the box initially contained fluid of a uniform density greater than the density of the ambient fluid. The experiment was started by removing one or more plugs from the lower openings. A plume is seen to descend from the box into the exterior from each opening. The volume flux out of the box due to the escaping fluid is balanced by the inflow of ambient fluid, which generates rising turbulent plumes within the box. The density of these plumes increases as they entrain fluid from their surroundings. On reaching the top of the box the fluid from the plumes spreads across the top before displacing denser fluid downwards: a circulation is thus set up within the box. The volume flux of this circulation is much greater than the volume flux out of the box and most of the fluid is recirculated within the plume. This recirculation ensures that fluid within the box is of roughly uniform density. Note, though, that this is only true if the depth of the box, H, is much greater than the lengthscale of the openings. An example of an experiment typical of the mixing flows is shown in figure 16. When, as in figure 16, more than one hole is open the flux through any one opening is primarily inflow or outflow with the sense of the flow changing periodically in time. This appears to be due to the interaction of the circulation within the box and the flow through the openings (see also Baines, Turner & Campbell 1990). Measurement of g' vs. t are shown in figure 17 and compared with the predictions of equation (3.3). The results agree well, though the rate of decrease of g' is slightly slower than expected.

Experiments conducted with the scale models were also in good agreement with the theory. In these cases the openings were in the sides of the boxes and so, as noted

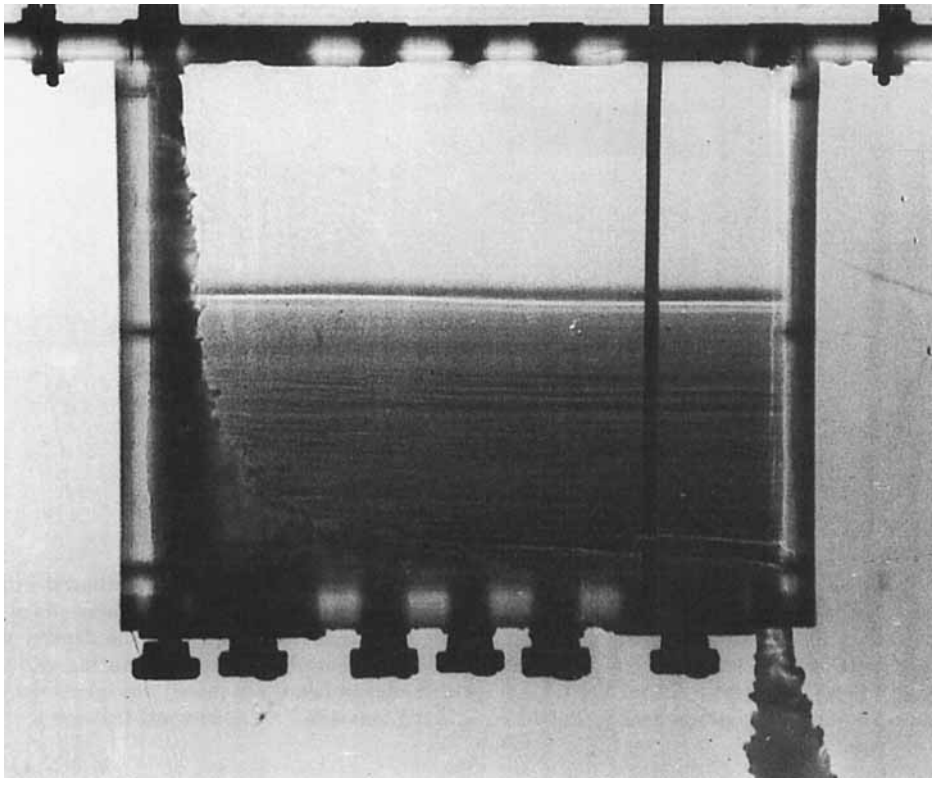

FIGURE 14. Steady displacement flow with a vertically distributed source. The source is against the left sidewall. Four large plugs from the top and one small plug from the bottom have been removed. Note the darkening of the fluid below the interface towards the floor and the horizontal lines showing variations in the stratification.

in §3, the exchange flow is greater resulting in a faster reduction of g' for a similar sized opening. When the openings were not at the bottom of the box, an interface formed at the level of the bottom of the windows. Fluid below the interface remained at its initial density and the density of the fluid above the interface decreased as predicted by the theory. Results from these experiments indicated that the rate of change of density does not increase linearly with the total area of openings as is expected. This is probably the result of the plumes occupying a larger fraction of the box as the number of openings is increased.

Internal sources

In this final set of experiments the fluid within the box was of the same density as the ambient fluid and dense fluid was introduced through a point source within the box. The development of the flow is illustrated in figure 18. A plume descends from the source creating a dense layer on the bottom of the tank as described in the section on displacement flows. The resulting exchange flow is very different, however. As the density of the fluid at the bottom of the box increases, an exchange flow is set up through the opening in the bottom similar to that discussed in the first part of this section. When there was a single opening in the bottom there was observed to be, once the steady state had been reached, an interface at $h/H \sim 0.3$. As more vents

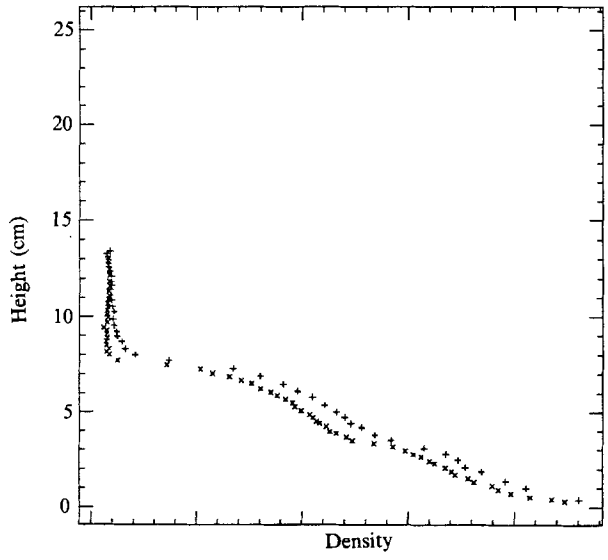

FIGURE 15. Density profile of a steady displacement flow with a vertically distributed internal source. This is from a steady state similar to that shown in figure 14. Here four large plugs from the top and three small plugs from the bottom have been removed. Note that the density is not uniform below the interface, nor is it uniformly stratified, having, rather, alternating regions of stronger and weaker stratification. The density (which has not been calibrated) was measured using a vertically traversing conductivity probe (+, upward traverse; ×, downward traverse).

were opened the interface moved towards the bottom, in accordance with the prediction of equation (3.7), and became more diffuse.

After some time a steady state is reached in which the source of buoyancy within the box is balanced by the outflow of dense fluid through the openings. The steady-state value of g' at the bottom of the box, g'_{E}, is then given by equation (3.5). The timescale for reaching the steady state is given by τ from equation (3.3), with $g'_0 = g'_{\mathrm{E}}$. Samples were taken in the lower half of the box in an experiment with a point source for various numbers of openings. The measurements corresponding to the steady states are shown in figure 19. The observed values of g' are less than the predictions of the theory, which suggests that the stratification is in fact more complex than the two-layer profile suggested by the analysis.

6. Applications to building ventilation

A major application of this work, as noted in the introduction, is to the natural ventilation of buildings. In this paper attention has been restricted to thermally driven flows, and the effects of wind have been ignored. The flows described above correspond both to the flushing of air out of an initially hot or cold space, and to the effects of continuous inputs (or the continuous removal) of heat. In temperate and hot climates natural ventilation is usually used during the summer months to remove the excess heat from the building. In this case the ambient air is usually warm enough to be introduced without pre-heating it and 'displacement ventilation' is an appropriate mode of ventilation. If the outside air is too cold, it can be mixed with the air in the building by introducing it through high level inputs using the 'mixing ventilation' mode.

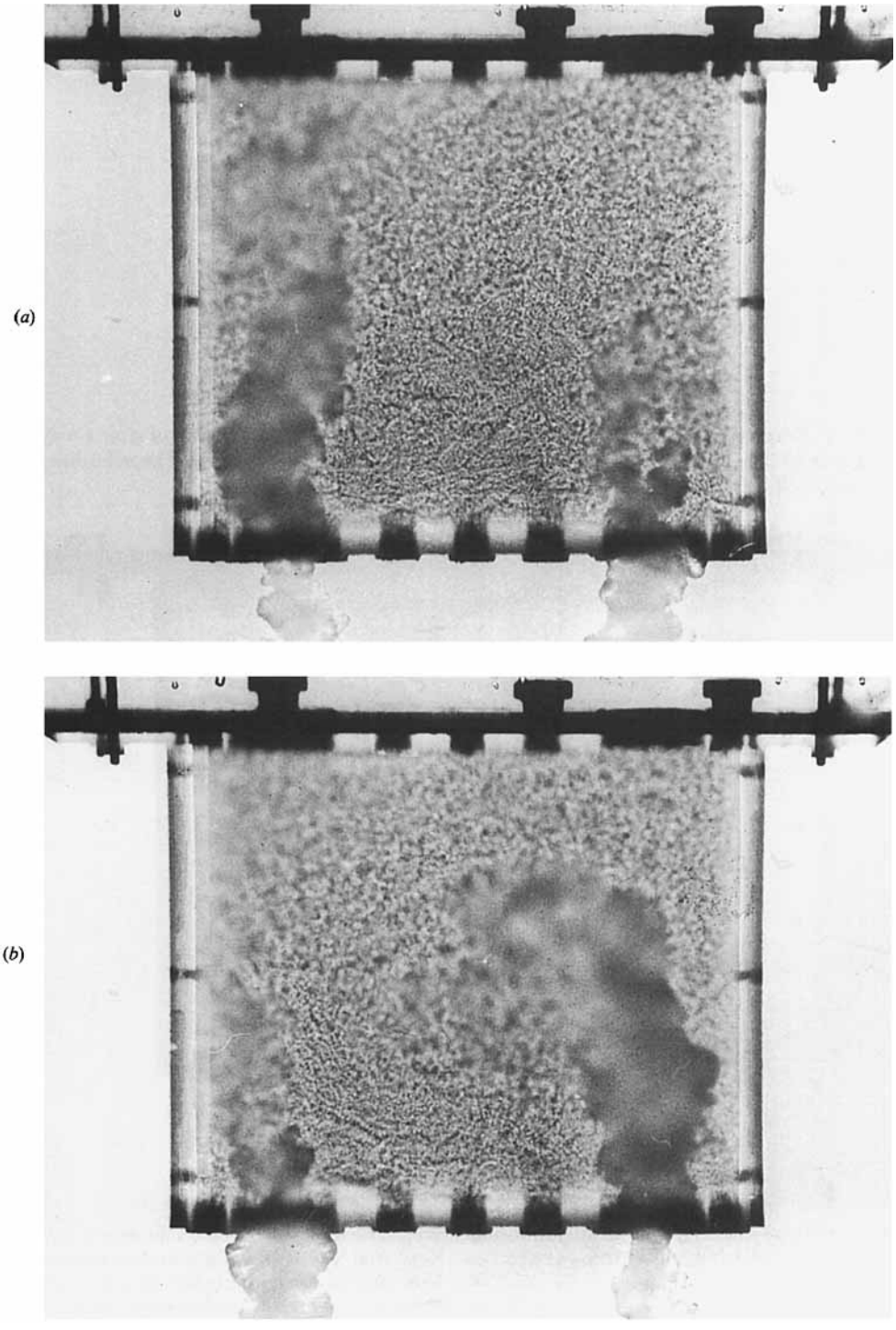

FIGURE 16. Mixing flow in a box initially containing dense fluid. The box was filled with dense fluid and placed in the large reservoir. The experiment was started by removing four large plugs from the bottom of the box. Note the intense mixing in the box and that the flow is largely in one direction through each opening, with flow in opposite directions through the left and right openings. The direction alternated over a period of about 5 s (compare *a* and *b*).

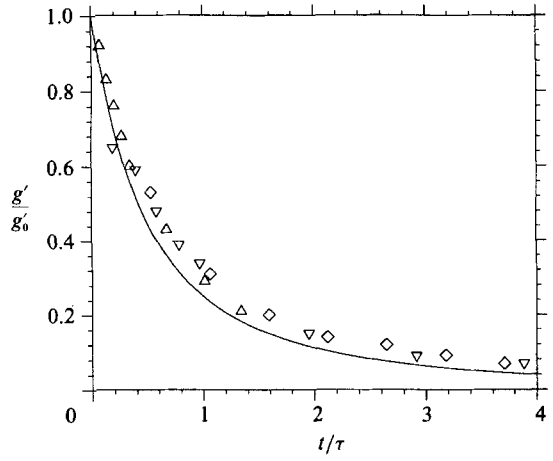

FIGURE 17. Emptying box by mixing flow: g'/g_0' *vs.* t/τ, where g_0' is the value of g' at $t = 0$ and τ is defined in (3.3*b*). Measurements were taken at mid-depth within the box. The solid line is the prediction of (3.3*a*).

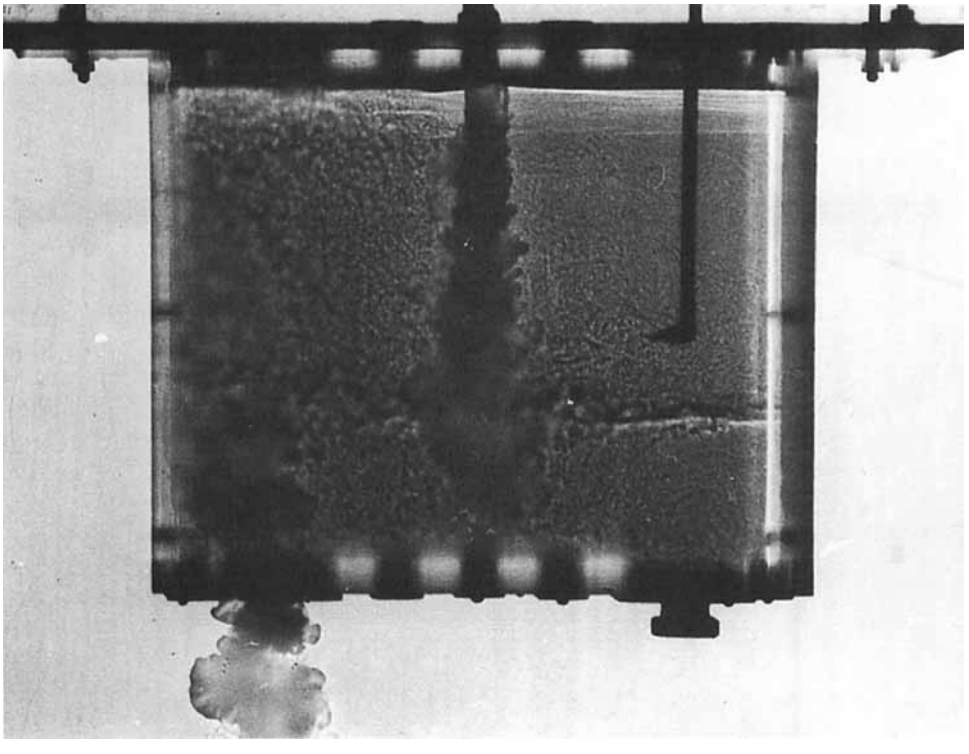

FIGURE 18. Steady mixing flow with an internal source. The source is a point source and one large plug was removed from the bottom of the box. Note that there is no interaction between the ascending and descending plumes within the box. Note also the sharp interface at approximately $\frac{1}{3}H$. There is little difference in the darkness of the fluid above and below the interface, showing that there is little change in the density. The measuring tip of the conductivity probe is at about $\frac{1}{2}H$.

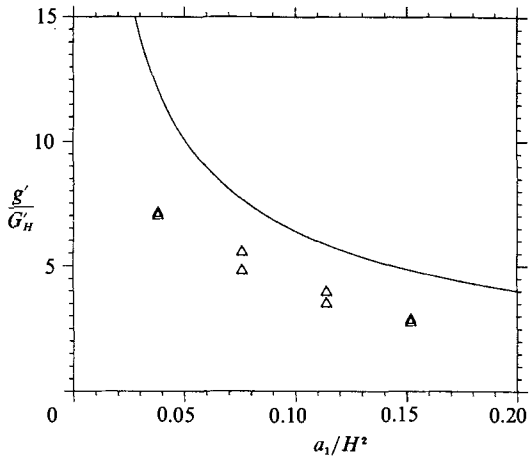

FIGURE 19. Mixing flow with a point source, g'/G'_H *vs.* a_1/H^2, where $G'_H \equiv G'(x = H, B)$ (see (2.9*c*)) and a_1 is the area of the openings in the bottom. The samples were taken from the lower half of the tank. The solid line is the prediction of (3.5) for the value of g' at the level of the openings.

In practice, most natural ventilation systems are a combination of the two modes. For example, the traditional sash-cord window when partially opened at the top and bottom allows inflow of cool air in the lower part and outflow of warm air through the upper part of the window. Typically, the upper part of the window is above head height and so this represents a displacement mode. However, the lower part of the window is usually 1 m or so above the floor, and cooler air which enters mixes to some degree with the air in the lower part of the room. On hot days it is most efficient to open both parts of the window, while if ventilation is required on cold days it is more comfortable to open only the top of the window to warm the incoming air by mixing. We see then that this traditional type of window is a versatile and efficient ventilation system.

In order to apply the results obtained in this paper to practical problems, it is necessary to scale the sources of buoyancy so that they correspond to the natural situation. The calculations and the experiments that we have made have been restricted to a very simple geometry and some idealized sources of buoyancy. Buildings have much more complicated shapes, with multiple zones and levels, and may be connected to the exterior by a number of different openings at different heights. The flows within these buildings are, in general, time-dependent and complex, and yet they are of crucial importance to the correct functioning of the building. In addition, in order to calculate heat losses and temperatures within the building the architect and the ventilation engineer need to have a knowledge of the internal flow patterns and the air movement.

The experiments we have described here provide a means of determining air movement and flow characteristics in complex buildings. A scaled model of the building is constructed and immersed in a tank of water. Dense salt solution is added to the model either to represent the initial temperature difference between the interior and the exterior air, or added continuously to represent inputs of heat, or a combination of both. If the air within the building is colder than the exterior air, the model represents the full-scale flow. If the air within the building is warmer than that outside, the model must first be inverted. When observed using an inverted camera, the correct view of the flow is obtained. An example of this technique is

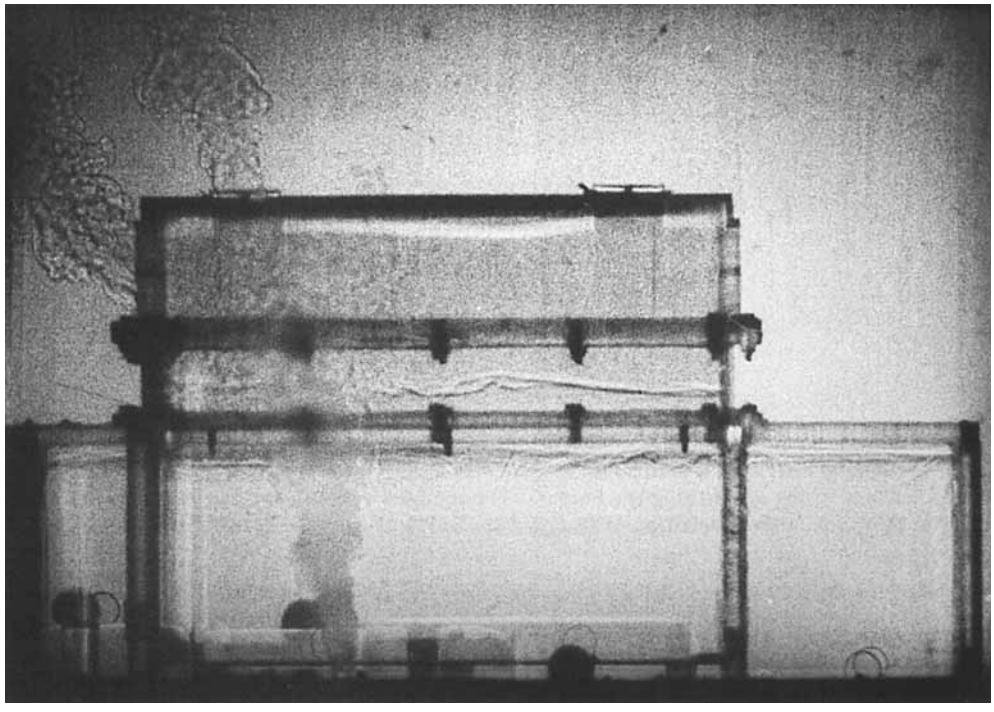

FIGURE 20. Displacement flow in a scale model of a building. The model is a 1:30 scale model of a courtroom, which has a raised roof over the central part of the court. Several vents near the floor, a window near the ceiling and a skylight are open.

given in figure 20. The photograph shows a 1:30 scale model of a proposed building for a Crown Court. Experiments have also been conducted with a 1:100 scale model of a section of the atrium of the proposed Westminster and Chelsea Hospital in London.

The flows are driven by buoyancy forces, which for a temperature difference ΔT are characterized by $g' = g\Delta T/T$, where T is the absolute temperature. As the dimensions of g' are lt^{-2}, we have

$$\frac{g'_{\text{model}}}{g'_{\text{full scale}}} = \frac{(lt^{-2})_{\text{model}}}{(lt^{-2})_{\text{full scale}}}.$$

Since the ratio of lengthscales is set by the model scaling, different model and real times are set by the ratio of g' between the laboratory and the real case,

$$\frac{t_{\text{full scale}}}{t_{\text{model}}} = \left(\frac{g'_{\text{model}}}{g'_{\text{full scale}}} \times \frac{l_{\text{full scale}}}{l_{\text{model}}}\right)^{\frac{1}{2}}. \tag{6.1}$$

Similarly, the velocities scale as

$$\frac{\text{velocity}_{\text{full scale}}}{\text{velocity}_{\text{model}}} = \left(\frac{(lg')_{\text{full scale}}}{(lg')_{\text{model}}}\right)^{\frac{1}{2}}. \tag{6.2}$$

For a continuous input of heat, with heat flux, W, the buoyancy flux $B = g\beta W/\rho c_p$, where β is the coefficient of expansion, ρ is the density and c_p is the specific heat. For a three-dimensional source the dimensions of B are l^4t^{-3}, and so equivalent scalings can be introduced for the laboratory scale.

There are two main advantages of modelling air flow ventilation using small-scale models in water. The first is that flow visualization is very straightforward, and complex flow patterns can be easily determined. The second advantage is that it is possible to use large values of g' (much larger values than is possible in air models) so that realistic Reynolds numbers and Péclet numbers may be realized (Linden & Simpson 1985; Lane-Serff 1989). Thus dynamic similarity is achieved. In addition, it is possible to make quantitative measurements of velocities and 'temperature' (salt concentration) distributions.

Another application of this work is to the flushing of gas out of a building after a gas leak. If displacement ventilation is used, there is no reduction in the maximum gas concentration during the flushing process, while mixing ventilation gives a spatially uniform reduction which will eventually bring the concentration below the flammable limit. The ratio of the timescales for the two modes of ventilation, given by (2.8) and (3.3*b*), is $t_E/\tau \approx k(d/H)^{\frac{1}{2}}$. Typically the size d of an opening is significantly less than the height of the building H, and, since $k = 0.25$ (vertical window) or $k = 0.05$ (horizontal vent), $t_E \ll \tau$. This suggests that the displacement mode is the most rapid means of removing the hazard.

Winds produce additional pressure differences and these may have quite different effects on the windward and leeward sides of buildings. A detailed discussion of these effects is beyond the scope of this paper, and we simply note here that for a building 5 m high with a difference in temperature of 10 °C between the interior and the exterior the resulting pressure difference is equivalent to a difference in velocity of approximately 1.3 m s^{-1}. Except on very calm days, wind speeds often exceed this value and so the effects of winds are likely to be important in most practical applications.

7. Conclusions

The fluid dynamics of natural ventilation have been investigated using simple mathematical models and laboratory experiments. We have restricted our attention to the case where the flows are driven by the hydrostatic pressure differences caused by density differences between the exterior and the interior fluid. Two ventilation modes have been identified: displacement ventilation where inflows occur at low levels and outflows occur at high levels, and mixing ventilation where the inflow of dense fluid occurs at high levels and mixes with the fluid in the interior. In displacement ventilation the interior is stably stratified, and vertical motions and mixing are small.

If the interior of the space is initially at a different density from the exterior and some vents are opened, the exchange flow replaces the interior fluid with exterior fluid. In the displacement case, the space empties in a time $t_E = (2S/A^*)(H/g')^{\frac{1}{2}}$. For a given geometry and initial density difference, the emptying time is controlled by the effective area A^* of the openings. From (2.4*b*) we see that A^* is dependent mainly on the smaller of the upper or lower level openings, and so control of the flushing rate is determined by the vents with the smaller total area. The implications of this for the removal of gas from an enclosure following a gas leak are discussed in §6. In the mixing ventilation mode the density of the fluid within the space approaches that of the exterior with a timescale which is inversely proportional to the area of the openings and k, the orifice coefficient (see (3.1) and (3.3*b*)). The value of k has been determined for vertical and horizontal vents, the latter being about 5 times less efficient than the former. However, the evaluation of k for horizontal vents has been

restricted to circular and square openings, and values for other shapes are not available.

With internal sources of buoyancy steady states are possible. In the displacement mode, sources at one level lead to a two-layer stratification. The height of the interface between the layers is determined solely by the area of the openings, the height of the space and the entrainment into the plume, and is independent of the buoyancy flux from the source. For a point source, an effective area of openings of $1/100$ of H^2 produces an interface at half-height, and a further increase by a factor of 10 is required to raise the interface to $0.9H$ (see (2.10) and figure 12). The densities of both layers are uniform, and the density difference across the interface is given by the density of the plume at the interface level (see (2.11*b*)). If the buoyancy flux from the source is doubled, the density difference increases by a factor of $2^{\frac{2}{3}} \approx 1.6$. Above the interface the plume becomes a pure momentum jet. Thus the connections with the exterior radically alter the filling box mechanism, and produce a very different internal stratification.

When the sources are distributed vertically, a more complicated stratification develops. Our theoretical calculations show that a layered density structure is established. The laboratory experiments show some indication of layers, but the observed scales are different from the predictions of §2.3. This discrepancy appears to result from the fact that the laboratory plumes are not as uniform across their cross-section as is assumed in the analysis. In addition the stratification is smoother than predicted; this is the result of mixing exterior to the plume. At full scale we expect the plume generated by, for example, solar heating of a wall to be more turbulent and that layered density stratification will develop.

In the mixing mode, the distribution of sources is less important in determining the steady state. However, if the ascending and falling plumes which are produced by the sources and the exchange flows, do not interact, a two-layer stratification develops. But, unlike the displacement flows, g' is non-zero in both layers and the stratification is weak. The precise conditions for the establishment of this stratification have not been determined.

The object of this paper has been to elucidate some aspects of the fluid mechanics of natural ventilation. A major result of our work is that the steady-state *form* of the stratification that develops in the space is determined solely by the distribution and sizes of the openings and the distribution and nature of the sources. This result holds for both displacement and mixing flows. If the strengths of the sources are increased then the magnitudes of the stratification and of the induced velocities are also increased, being proportional to the two-thirds power and one-third power of the buoyancy flux, respectively; but the flow patterns and the shape of the density profile remain unchanged.

In practice, ventilation flows are turbulent, unsteady and three-dimensional, and it is not possible to make accurate theoretical or numerical calculations of these flows. The limitations of fully three-dimensional calculations are even more severe when the geometry of the ventilated space is complex. The approach we have adopted is in the spirit of 'zone models' where the elements of the flow are parameterized in some way. We have considered the effects of sources of buoyancy, which we have modelled as producing turbulent plumes, and have parameterized the turbulent processes using the entrainment assumption of Morton *et al.* (1956). The main limitation on the applicability of our results is then determined by the accuracy of treating buoyancy inputs in this way. The agreement between the calculations and the laboratory experiments provides confidence that this parameterization is an accurate one.

The main remaining question concerns the approximation of real inputs of buoyancy as plumes arising from point, line or area sources. The conditions under which a group of individuals in a room can be considered as independent sources or as a distributed area source are not known. Solar heating of a wall produces a turbulent boundary layer, and the effects of the detailed structure of this flow need further study.

This work has evolved from collaboration with Dr F. Penz at the Martin Centre for Architectural and Urban Studies, University of Cambridge, with whom we have enjoyed many illuminating discussions on the architectural problems of ventilation. P.F.L.'s original interest in the fluid mechanics of ventilation was sparked by George Batchelor several years ago when he suggested I attend some discussions with the Departments of Architecture and Engineering on questions of energy use and conservation in buildings. We have been inspired by George's early work on similarity theories of plumes, and on the fluid mechanics of double-glazed windows, and would like to think that this paper continues the spirit of that work.

Our work in ventilation has been funded in part by British Gas PLC and we acknowledge the support of Dr R. Hitchin and Dr M. Marshall. G.F.L.-S. is supported by a British Gas Research Scholarship. The work on the Crown Court design and the Westminster and Chelsea Hospital was funded by the Property Services Agency and Sheppard Robson Ltd, respectively.

The models were designed and built by D. Cheesely, D. Lipman, E. Maclagan and P. O'Reilly.

REFERENCES

BAINES, W. D. & TURNER, J. S. 1969 Turbulent buoyant convection from a source in a confined region. *J. Fluid Mech.* **37**, 51–80.

BAINES, W. D., TURNER, J. S. & CAMPBELL, I. H. 1990 Turbulent fountains in an open chamber. *J. Fluid Mech.* **212**, 557–592.

BATCHELOR, G. K. 1967 *An Introduction to Fluid Dynamics*. Cambridge University Press.

BROWN, W. G., WILSON, A. G. & SELVASON, K. R. 1963 Heat and moisture flow through openings by convection. *J. Am. Soc. Heating Ventilation Air Conditioning Engng* **5**, 49–54.

DALZIEL, S. B. 1988 Two-layer hydraulics – maximal exchange flows. Ph.D. thesis, University of Cambridge.

EPSTEIN, M. 1988 Buoyancy-driven exchange flow through openings in horizontal partitions. *Intl Conf. on Cloud Vapor Modelling. Nov. 1987, Cambridge, MA*.

LANE-SERFF, G. F. 1989 Heat flow and air movements in buildings. Ph.D. thesis, University of Cambridge.

LINDEN, P. F. & SIMPSON, J. E. 1985 Buoyancy driven flows through an open door. *Air Infiltration Rev.* **6**, 4–5.

MORTON, B. R., TAYLOR, G. I. & TURNER, J. S. 1956 Turbulent gravitational convection from maintained and instantaneous sources. *Proc. R. Soc. Lond.* **A234**, 1–23.

PENZ, F. A. 1983 Passive solar heating in existing dwellings. *ETSU publication* ETSU-5-1056a.

PENZ, F. A. 1986 A monitoring exercise in a school atrium. *Appl. Energy* **22**, 1–13.

WORSTER, M. G. & HUPPERT, H. E. 1983 Time-dependent profiles in a filling box. *J. Fluid Mech.* **132**, 457–466.